SUPPLEMENTARY FIGURES ONLINE

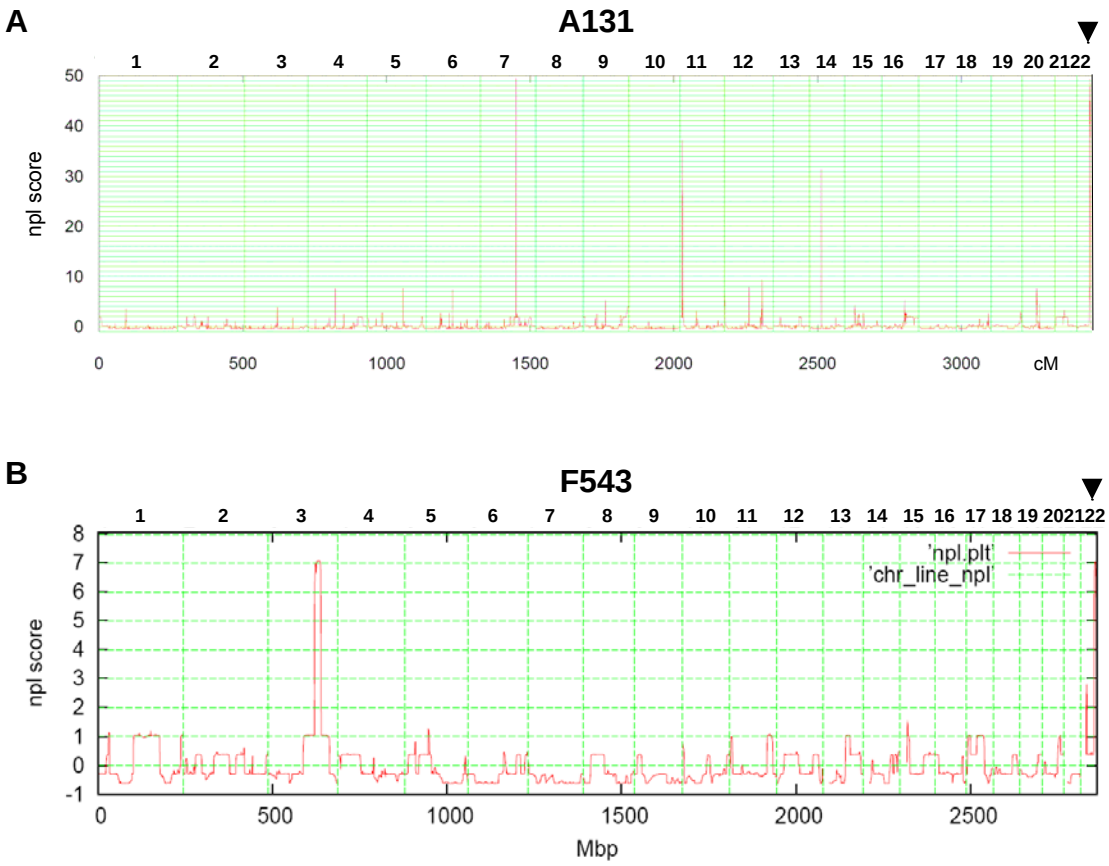

Supplementary Fig. 1. Whole genome search for linkage by homozygosity mapping in two remotely consanguineous families with NPHP using 50k SNP arrays.
Family A131 from Northern Finland has 3 affected individuals. Family F543 from Turkey has 2 affected individuals. Graphs represent non-parametric LOD scores (NPL) on the y-axis in relation to genetic position on the x-axis. Human chromosomes are concatenated form p-ter (left) to q-ter (right) on the x-axis. Genetic and physical distances are given in cM for NPL calculation with ALLEGRO (**A**) and in Mbp for GENEHUNTER (**B**). NPL peaks represent regions of putative homozygosity by descent, indicating candidate loci. No mutations were detected by direct exon sequencing of every gene contained with in the peak on chromosome 7 (**A**). Note that the presence of an overlapping peak on chromosome 22q for both kindred (arrow heads) was detected at the *NPHPL1* locus. The maximum parametric LOD score in A131 was 3.6 (see **Fig. 2**).

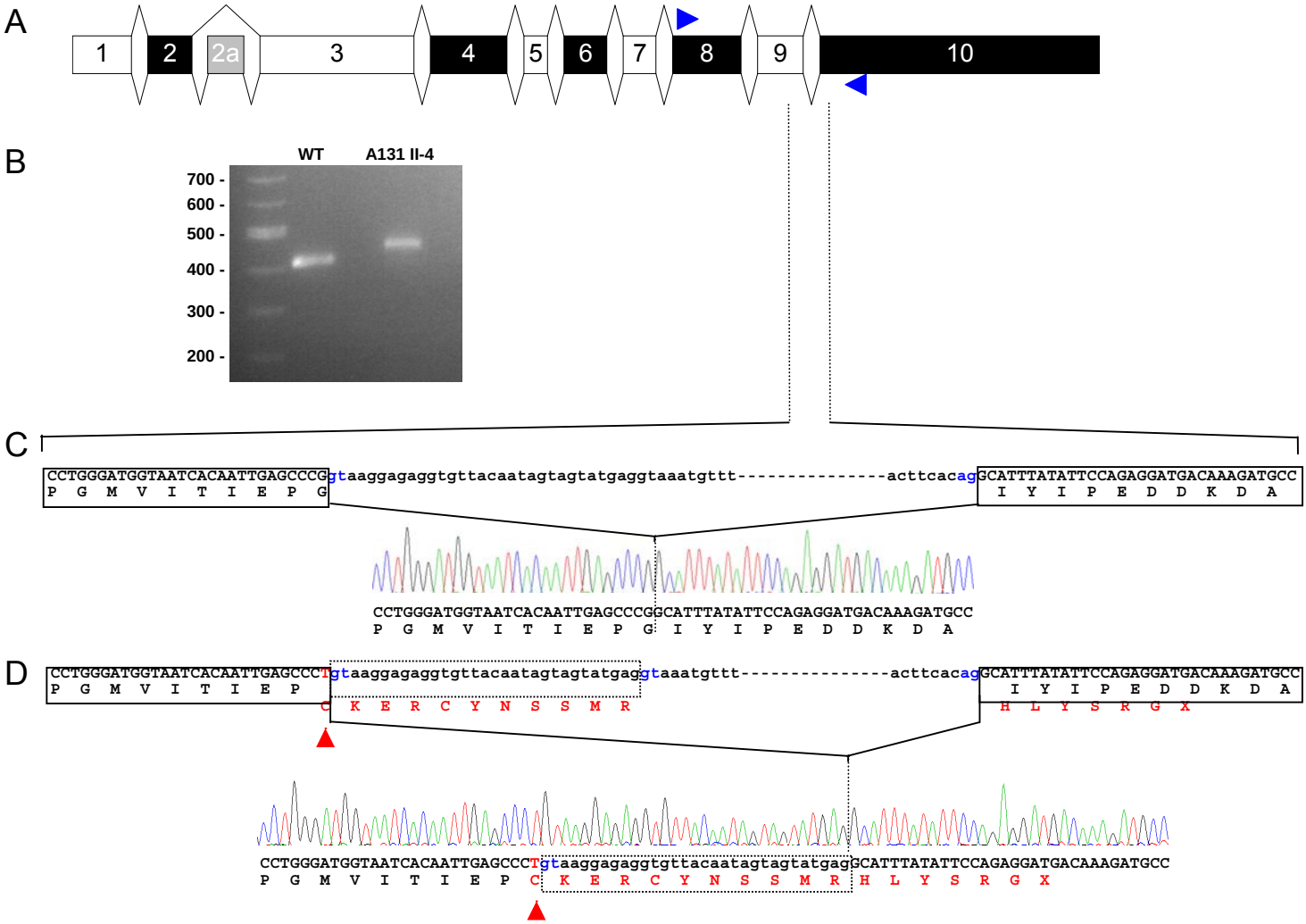

Supplementary Figure 2. Homozygous splice site mutation (c.1357G>T) of the last base of exon 9 in family A131. (**A**) Exon structure of *XPNPEP3* with alternative splicing of exon 2a. (**B**) RT-PCR using exonic primers (blue arrowheads in **A**) was performed in a healthy control and in affected individual A131 II-4, who is homozygous for the mutation c.1357G>T (p.453G>C, conserved in *E. coli*). This last base of exon 9 is 80% conserved within the splice donor consensus. RT-PCR yielded a wild type band (WT) of 430 bp in a healthy control individual and a single band at ~460 bp in A131 II-4. Both bands were excised and directly sequenced and demonstrated normal splicing between exons 8 and 9 (not shown). Note that there is an additional faint band at the size of the wild type splice product for affected individual A131-II4, potentially indicating some residual correct splicing. (**C-D**) Sequences of WT and mutant at the exon 9 to 10 splice site. Boxes encase the exon nucleotide sequence above amino acid sequence. Obligatory splice donor and splice acceptor bases are in blue. The mutated nucleotide (c.1357G>T) and resultant amino acid sequence are in red. Intron sequence is in lower case, exon sequence in upper case. (**C**) Partial genomic wild type sequence of the healthy control is shown above partial cDNA wild type sequence. The wild type splice junction is indicated by a vertical dotted line. (**D**) Partial genomic sequence of the affected individual A131 II-4 is shown above partial cDNA sequence. The mutated nucleotide is colored in red. A dashed box surrounds 31 additional nucleotides of intron 9 that are included in the transcript of A131 II-4 due to skipping of the mutated splice donor site and activation of a cryptic splice donor. The resultant amino acid sequence (red) encounters a stop codon (p.470X) seven amino acids residues into exon 10 due to a frame shift. This truncates the last 38 amino acid residues of the prolidase domain of the protein, which demonstrates high amino acid sequence conservation to *E. coli*.

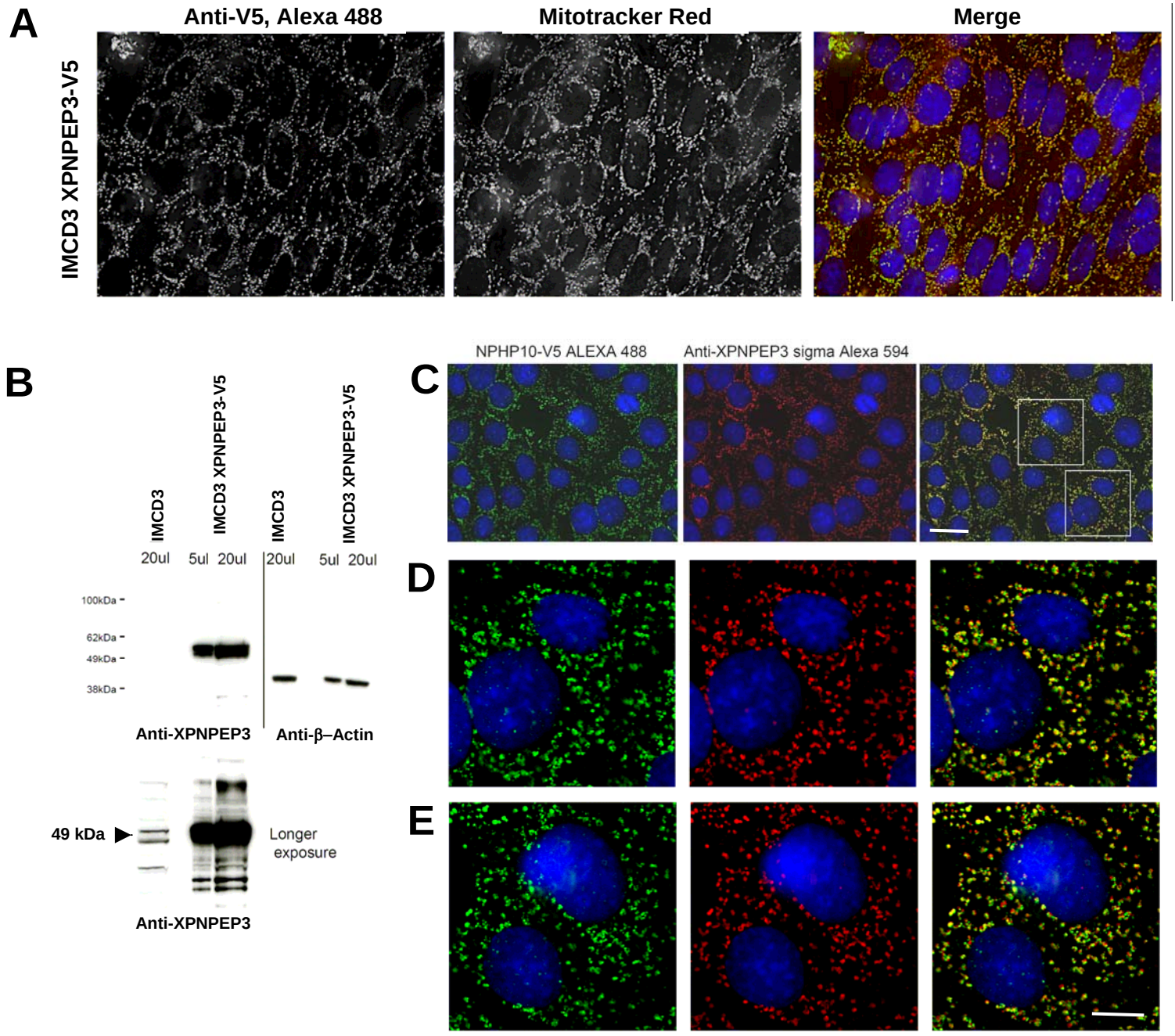

Supplementary Figure 3. The rabbit polyclonal α-XPNPEP3 antibody HPA000527 (Sigma) is specific for XPNPEP3 and locates it in mitochondria.

(**A**) Stably expressed full-length human XPNPEP3-V5 detected with an anti-V5 antibody (left panel) fully colocalizes (right panel) with the mitochondrial marker "mitotracker red" (middle panel), thereby demonstrating mitochondrial localization of XPNPEP3. Scale 20 μm.

(**B**) Western blot of recombinant V5-tagged full-length human XPNPEP3 stably expressed in IMCD3 cells. The α-XPNPEP3 antibody detects XPNPEP3-V5 at the expected size of 51 kDa (left panel). An anti-actin antibody is used as loading control (right panel). In untransfected IMCD3 it also detects two bands at 48 kDa and 51 kDa.

(**C**) Immunofluorescent microscopy in IMCD3 cells that stably express full-length human XPNPEP3-V5 using an anti-V5 antibody (left panel) yields a mitochondrial expression pattern. It fully colocalizes (right panel) with the pattern generated by the α-XPNPEP3 antibody (middle panel), thereby confirming its specificity for XPNPEP3. **(D,E,)** Higher magnification (scale 10μm) of areas delineated by the insets shown in (**C**).

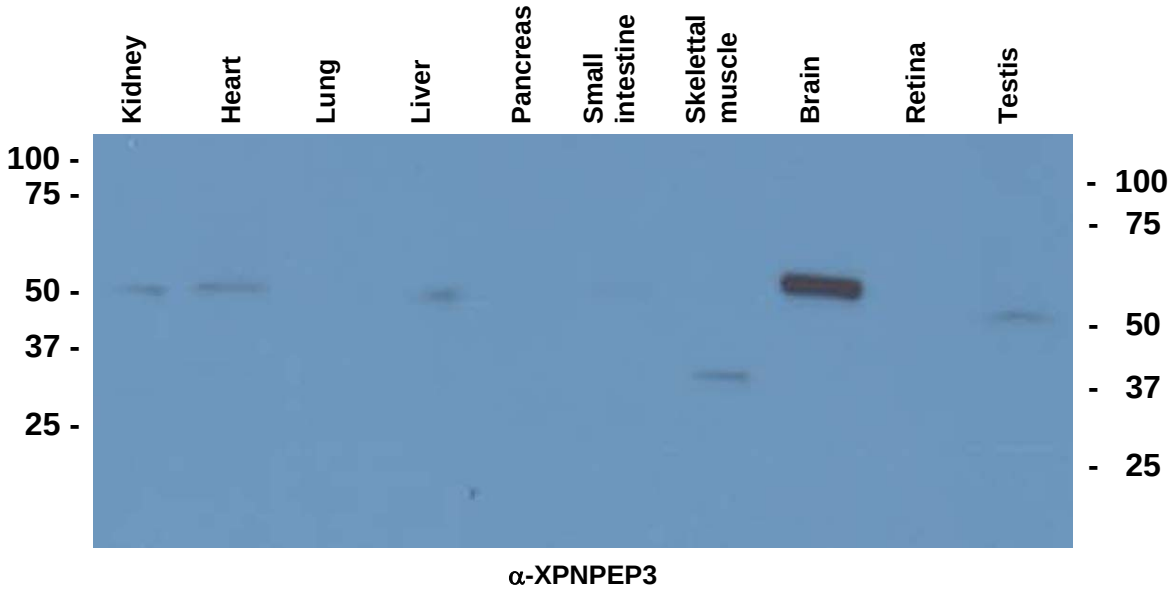

Supplementary Figure 4. Characterization of *XPNPEP3* expression in multiple tissues from mouse by immunoblotting. α-XPNPEP3 recognizes single bands at 51 kDa in cell lysates of kidney, heart, liver, and testis (most likely representing the cleaved isoform 1 of XPNPEP3; see **Fig. 2**), a band of 57 kDa in brain (most likely representing the uncleaved isoform 1 of XPNPEP3), and short band in skeletal muscle (potentially representing the product of splice isoform c; http://www.ncbi.nlm.nih.gov/IEB/Research/Acembly/). A duplicate blot incubated with the secondary antibody alone as negative control did not reveal any bands (data not shown).

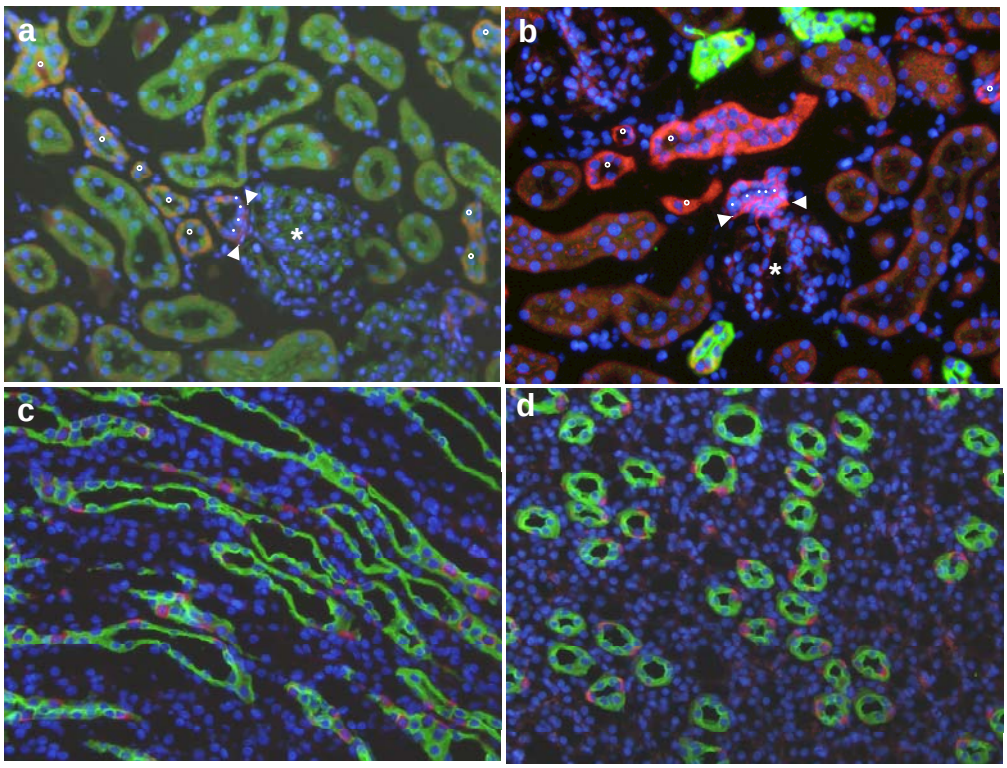

Supplementary Figure 5. XPNPEP3 is expressed in distal convoluted tubule (DCT) and cortical collecting duct (CCD) in rat kidney.

(**a-b**) Immunofluorescence with the α-XPNPEP3 antibody (red) yielded cell-specific basolateral expression of XPNPEP3 in DCT (white circles). High expression of XPNPEP is present in lacis cells (extraglomerular mesangial cells demarcated between arrow heads) adjacent to the macular densa (shown by blue nuclei marked by with dots). There is also weak expression in proximal tubule cells. Nuclei are stained with DAPI (blue). Cells were counterstained (green) with mitochondrial marker CytCox (**a**), and with CCD marker AQP2 (**b**-**d**). (**c**-**d**) In the renal medulla XPNPEP3 (red) is expressed basolaterally in intercalated cells, which are also known as “dark cells” due to their abundance of mitochondria. Principal cells, counterstained with AQP2 (green), are XPNPEP3 negative.

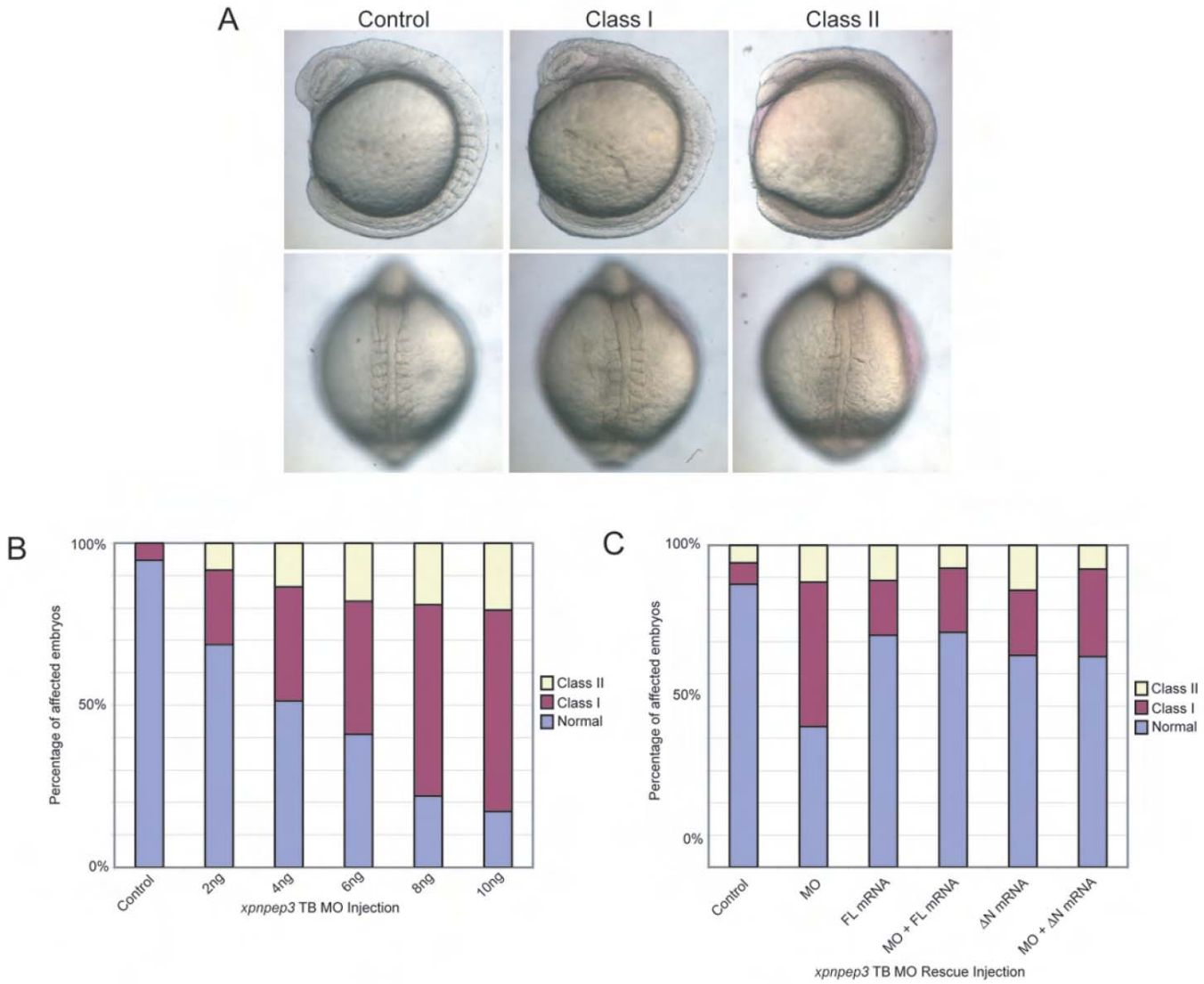

Supplementary Figure 6. XPNPEP3 suppression phenocopies ciliary zebrafish morphants
A. *xpnpep3* morphants display defective gastrulation movements. Lateral and dorsal views of representative Class I and Class II *xpnpep3* morphants at the 8-10 somite stage.
B. *xpnpep3* morpholino (MO) dose response curve. A translation-blocking morpholino was designed against the *Danio rerio* ortholog of human XPNPEP3, and was injected at increasing concentrations into zebrafish embryos at the two-cell stage (n = 100 embryos/injection) to assess MO efficiency. Embryos were then phenotyped at the 8-10 somite stage for developmental defects with the experimenter blinded to injection. Class I embryos are mildly affected and display shortening and thinning of the body axis, a slightly smaller head, and minor to no somitic or notochord defects. Class II embryos are severely affected and are characterized by a short and thin body, small head, a broadened and/or kinked notochord, and broad, thin somites. Similar results were observed with an *xpnpep3* splice-blocking MO (data not shown).
C. Rescue of the detrimental effects of *xpnpep3* MO with human *XPNPEP3* mRNA. Embryos were injected at the two-cell stage with either 4 ng MO, 50 pg human mRNA, or 4 ng MO plus 50 pg human RNA and were then phenotypically scored at the 8-10 somite stage (n = 100 embryos/injection). MO rescue with either full-length (FL) mRNA or transcript lacking the mitochondrial leader sequence (ΔN) resulted in similar rescue efficiencies (FL vs ΔN rescue; χ^2= 3.470, p= 0.1764).

Supplementary Table 1. *XPNPEP3* exon primers. Primer names, sequences, and product length in bp are given. Forward primers were used for PCR product sequencing.

DL65_XPNPEP3ex1_F	GGCATGACGTCACAACCTG	394
DL66_XPNPEP3ex1_R	ACCCCTTTCCAGGAGCAG	394
DL73_XPNPEP3ex2_F	TGAATATTGAAGGAGAGAAGGAAG	387
DL74_XPNPEP3ex2_R	AATGGCCATGTGAGGTTAGTG	387
DN41_XPNPEP3ex2b_F	CACATTGTAGAAAAAGCAATCAGG	475
DN42_XPNPEP3ex2b_R	TTAAGGCCTGGAAAATGCAG	475
DL75_XPNPEP3ex3_F	TGTGCTGTGAGGAGATTTGG	661
DL76_XPNPEP3ex3_R	CTTTCATGGTGCTCATGGTC	661
DL77_XPNPEP3ex4_F	GTTTAGGGGCAGAAAAGCTG	840
DL78_XPNPEP3ex4_R	GTATACGACCTCAAGAGCTTACG	840
DL79_XPNPEP3ex5_F	AACTTCAGGCTGACGAAATTG	304
DL80_XPNPEP3ex5_R	TCCTCTCCAATGACATGCTG	304
DL81_XPNPEP3ex6_F	GGGGTGAGAATAAAAGAAATGG	500
DL82_XPNPEP3ex6_R	GAGGCATGTTAATAATTCCTCCTAAC	500
DL83_XPNPEP3ex7_F	GCAACAAGAGTGAAACTCCG	330
DL84_XPNPEP3ex7_R	TTGCAACCTAACTTGACCAGG	330
DL85_XPNPEP3ex8_F	AAACATCAACAGTGCCCCAG	445
DL86_XPNPEP3ex8_R	TGCCTCAGCCTCCTAAACTAC	445
DL87_XPNPEP3ex9_F	TTAAACTGAAGTGGCAGAACC	391
DL88_XPNPEP3ex9_R	GAATTGCTGAACCTGGGG	391
DL89_XPNPEP3ex10_F	ACTAGGTAGGTACCATAAAGATCCAG	427
DL90_XPNPEP3ex10_R	TCACACAGCTGCTATGCTCC	427

Supplementary Table 2. Mitochondrial respiratory chain complex (RCC) enzyme activities in skeletal muscle biopsy of individual A131-II with homozygous *XPNPEP3* mutation (c.1357G>T, p.G453C).

Respiratory chain span	Activity (nmol/min/mg)	Normal range (nmol/min/mg)	Relative to Succ→Cyt *c*	Relative to Citrate synthase (1000×)
NADH → Q[a]	210	85-337	1.18	0.40
NADH → Cyt *c*[b]	146	104-312	0.82	0.28
Succ → Cyt *c*[c]	178	126-443	1	0.34
QH_2 → Cyt *c*[d]	257	105-406	1.45	0.50
Cyt *c* → O_2[e]	273	137-1007	1.54	0.53

[a]NADH: ubiquinone oxidoreductase (decylubiquinone as substrate)
[b]NADH:cytochrome *c* oxidoreductase
[c]Succinate:cytochrome *c* oxidoreductase
[d]Ubiquinol:cytochrome *c* (decylubiquinol as substrate)
[e]Cytochrome *c* oxidase

Supplementary Table 3. Mitochondrial DNA content and morphology in skeletal muscle biopsy of individual A131-II.

	MtDNA amount referenced to nuclear DNA[a] (relative to age-matched control)	Deletions[b]	Electron microscopy
Mitochondrial DNA	0.71	None	
Mitochondrial aggregates			None
Fat accumulation			None

[a]At the age of 17 yrs. The mitochondrial *ND1* gene references to the nuclear encoded *brain natriuretic peptide* (*BNP*) gene (He L et al. *Nucleic Acids Res* 2002;30:e68).
[b]Analyzed by means of long PCR using the "Expand Long Template PCR" System kit (Boehringer-Mannheim).

Supplementary Table 4. Mitochondrial respiratory chain enzyme activities in skeletal muscle biopsy sample from individual F543-I with homozygous *XPNPEP3* mutation p.N311LfsX5.

Respiratory chain span	Activity (U/g NCP)	Normal range (nmol/min/mg)	U/U CS	Normal range (U/U CS)
NADH → Q[a]	6.5	12.0-26.4	0.14	0.17-0.56
Succ → Cyt *c*[c]	10.2	6.0-25.0	0.21	0.08-0.45
Cyt *c* → O_2[e]	92	112-351	1.9	1.1-5.0

[a]NADH: ubiquinone oxidoreductase (decylubiquinone as substrate)
[c]Succinate: cytochrome *c* oxidoreductase
[e]Cytochrome *c* oxidase

Supplementary Table 5. Mitochondrial DNA (mtDNA) and morphology in skeletal muscle biopsy sample from idividual F543-I with a homozygous *XPNPEP3* mutation p.N311LfsX5).

.	MtDNA amount referenced to nuclear DNA[a] (relative to age-matched control)	Deletions[b]	Electron microscopy	Histology	MELAS (3243,13513) tRNA: Leu, Ser, Lys Mutation
Mitochondrial DNA	<0.1 (normal range 0.2-1)	None			none
Mitochondrial aggregates			None	None	
Fat accumulation			None	None	

[a]Investigated by *Pvu*I restriction and Southern blot analysis.
In addition, the mtDNA screening of all RCC I subunits (ND1, 2, 3, 4, 4L, 5, 6) and all tRNA genes revealed no potential pathogenic mutation as well as the screening of all nuclear encoded RCC I subunits and known assembly factors (n=50 genes).

I

Supplementary Table 6. Mitochondrial respiratory chain enzyme activities in a fibroblast cell culture from individual F543-II skeletal muscle biopsy sample from individual F543 with homozygous *XPNPEP3* mutation p.N311LfsX5.

Respiratory chain span	Activity (U/g NCP)	Normal range (nmol/min/mg)	U/U CS	Normal range (U/U CS)
NADH → Q[a]	5.55	10.75-17.72	0.06	0.10-0.27

[a]NADH: ubiquinone oxidoreductase (decylubiquinone as substrate)

There is a pronounced RCC I defect reflected by a reduction of activity of NADH: ubiquinone oxidoreductase (decylubiquinone as substrate) to 60%.

Supplementary Table 7. O_2 flux (pmol/(s*Mil)) in permeabilized fibroblasts from individual member F543-II (black) and healthy control subjects (white). Data (means±SD) are shown as O_2 flux per 10*6 cells. (***$p < 0.001$).

Substrates	Maximal ADP stimulated respiration (state 3) O_2 flow per cells [pmol/(s*Mil)]	Normal range of maximal ADP stimulated respiration (state 3) O_2 flow per cells [pmol/(s*Mil)]
Glu+Mal → O_2	78[a]	103-126
Succ → O_2	97	100-140
TMPD+Asc → O_2	180	173-212

[a]Oxygene consuption with RCC I substrates (glutamate/malate) shows an activity of only 76 % of the lowest value of the control range. Oxygene consuption with succinate (RCC II substrate) is at the lower range of control subjects.

Supplementary Table 8. Putative ciliary targets of XPNPEP3. Proteins that have a proline in the second position (after initiation methionine) were parsed from the ciliary proteome (www.ciliaproteome.org) from the reciprocal orthologs with an E-value <e-30.

Accession number	Gene name	N-term peptide sequence	Number of proteomics studies
O15078	CEP290	MPPNINWKEI	9
Q9BVG8	KIFC3	MVPSRRTWNL	9
Q07283	TCHH	MSPLLRSICD	8
Q5VTH9	WDR78	MTPGKHSGAS	8
Q9H0U4	RAB1B	MNPEYDYLFK	8
Q9UI46	DNAI1	MIPASAKAPH	8
O95995	GAS8	MAPKKKGKKG	7
O14645	DNALI1	MIPPADSLLK	6
P09211	GSTP1	MPPYTVVYFP	6
P30085	CMPK	MKPLVVFVLG	6
Q8IWG1	WDR63	MAPKQKKKTS	6
Q8TES7	FBF1	MAPKTKKGCK	6
Q9UBS4	DNAJB11	MAPQNLSTFC	6
P22105	TNXB	MMPAQYALTS	5
P54819	AK2	MAPSVPAAEP	5
Q8NEP3	LRRC50	MHPEPSEPAT	5
Q96MC2	C2orf39	MNPPGSLEAL	5
P39060	COL18A1	MAPYPCGCHI	4
Q0VAA2	C14orf166B	MPPDEIEIEP	4
Q13347	EIF3I	MKPILLQGHE	4
Q8WVS4	WDR60	MEPGKRRTKD	4
Q99832	CCT7	MMPTPVILLK	4
Q9Y6Q1	CAPN6	MGPPLKLFKN	4
P11166	SLC2A1	MEPSSKKLTG	3
P13667	PDIA4	MRPRKAFLLL	3
P21589	NT5E	MCPRAARAPA	3
P50502	ST13	MDPRKVNELR	3
Q07960	ARHGAP1	MDPLSELQDD	3
Q5JU67	C9orf117	MAPKKSVSKA	3
Q8TC29	C10orf63	MDPTCSSECI	3
Q9BS26	TXNDC4	MHPAVFLSLP	3
Q9BZH6	BRWD2	MLPYTVNFKV	3
Q9C005	DPY30	MEPEQMLEGQ	3
Q9H8T0	AKTIP	MNPFWSMSTS	3
Q9HD45	TM9SF3	MRPLPGALGV	3
O43237	DYNC1LI2	MAPVGVEKKL	2
O77932	DOM3Z	MDPRGTKRGA	2
P11586	MTHFD1	MAPAEILNGK	2
P11831	SRF	MLPTQAGAAA	2
P11940	PABPC1	MNPSAPSYPM	2
P16473	TSHR	MRPADLLQLV	2
P22087	FBL	MKPGFSPRGG	2
Q15021	NCAPD2	MAPQMYEFHL	2
Q68DX3	FRMPD2	MQPLTKDAGM	2
Q6NUP7	KIAA1622	MHPPPPAAAM	2
Q7Z460	CLASP1	MEPRMESCLA	2
Q86T82	USP37	MSPLKIHGPI	2
Q8IWT6	LRRC8A	MIPVTELRYF	2
Q8IWU9	TPH2	MQPAMMMFSS	2
Q8TCU4	ALMS1	MEPEDLPWPG	2
Q96LD8	SENP8	MDPVVLSYMD	2